CFD Letters www.cfdl.issres.net Vol. 6 (1) – March 2014

Numerical Simulation of Double Diffusive Laminar Mixed Convection in a Horizontal Rotating Annulus

Part (I): Effect of Richardson and Lewis numbers

Medhat M. Sorour [1],Mohamed A. Teamah [2], Wael M. El-Maghlany [11], Heba M. Abdel Aziz [3]
[1] *Mechanical Engineering Department, Alexandria University*
Alexandria, EGYPT
[2]*Arab Academy for Science, Technology and Maritime Transport*
Alexandria, EGYPT
[4] *Alexandria Higher Institute for Engineering and Technology*
Alexandria, EGYPT

Received: 04/08/2013 – Revised 13/12/2013 – Accepted 14/03/2014

Abstract

A numerical study of double-diffusive mixed convection within a horizontal rotating annulus has been investigated. The outer cylinder is fixed but the inner cylinder is considered to rotate in clockwise and anti-clockwise directions to introduce the forced convection effect. In addition, the solutal and thermal buoyancy forces are sustained by maintaining the inner and outer cylinder at uniform temperatures and concentrations but their values for the inner are higher than the outer. The flow is considered laminar regime under steady state conditions. The transport equations for the continuity, momentum, energy and mass transfer are solved using the finite volume technique. The considered domains in this investigation are: $0.01 \leq Ri \leq 100$ and $0.01 \leq Le \leq 100$. While the thermal Grashof number, Prandtl number, buoyancy ratio and the radius ratio are kept constant at values equal to10^4, 0.7, 1 and 2 respectively. The effect of the selected parameters on the local and average Nusselt and Sherwood numbers are presented and studied. Finally, this investigation concerned with selection the best direction of the inner cylinder rotation to enhance both heat and mass transfer. A comparison was made with the published results and a good agreement was found.

Keywords: Double-diffusive flow; Mixed heat and mass transfer; Rotating annulus.

1. Introduction

When the fluid flow is induced by the combination of temperature and concentration gradients, double diffusion convection is found. Double-diffusion convection in confined spaces has a lot of attention in the investigation field because of its wide engineering and industrial application. One of these applications is the technologies involved in the chemical vapor deposition processes for the semiconductors device fabrications.

[C] Corresponding Author: Wael M. El-Maghlany
Email: elmaghlany@yahoo.com Telephone: +201223741891 Fax: +2035921853
 PII: S2180-1363(14)6032-X

The migration of the species is known to be sensitive to the magnitude of rotational speed, which is a crucial parameter in drying technologies, printing and crystal growth applications. Other technologies including melting and solidification processes in rotating furnace are likely candidates for such applications. A series of numerical studies for the natural and mixed convection heat transfer in a horizontal rotating annulus were conducted by Joo-Sik Yoo and coworker [1-3], these studies cover a wide range of Grashof number, Prandtl number and the radius ratio. He studied the transitions in flow from two eddies to one eddy and from one eddy to no-eddy. In addition, several studies were reported on the natural convection heat transfer in a horizontal annulus. Gilles et al. [4] studied the effect of the thermal Rayleigh number and the radius ratio on the thermal and hydrodynamic instabilities for air filled annuli. Hamad and Khan [5] investigated experimentally the natural convection in a cylindrical annulus to study the effect of angle of inclination and diameter ratio on heat transfer and empirical correlations for the average Nusselt number as a function of Rayleigh number were given for different radius ratios and angles of inclination. Also the natural convective heat transfer was investigated between two horizontal, elliptic cylinders numerically by Zhu et al [6], through this study, Rayleigh number was fixed at 10^4, Prandtl number at 0.7, the radius ratio at 2.6 and vertical and horizontal orientations were taken for either the outer or the inner cylinder to see their behaviors on both streamlines and heat transfer. Abu-Nada et al. [7] investigated the heat transfer enhancement in horizontal annuli using nano-fluids, water-based nano-fluid containing various volume fractions of *Cu*, *Ag*, Al_2O_3 and TiO_2 nano-particles were used. For the mass transfer, Bowman and Schwartz [8] investigated the mass transfer rate numerically for high Peclet number acoustic streaming flow between two concentric cylinders where a harmonic oscillation was imposed to the outer cylinder. For the double diffusion mixed convection problems, comprehensive reviews on the study of double diffusive laminar mixed convection in a horizontal annulus with hot, solutal and rotating inner cylinder were presented by Teamah [9], the following parameters were kept constant: Prandtl number at 0.7, the rotational Reynolds number at 100 and the radius ratio at 2. Usefully correlations for both average Nusselt and Sherwood numbers were introduced, but in his study the value of Reynolds is fixed and the Richardson number change with the change in Grashof number. A numerical investigation of mixed convection in a horizontal annulus filled with a uniform fluid-saturated porous medium in the presence of internal heat generation was carried out by Khanafer and Chamkha [10]. Cheng [11] examined the effects of the modified Darcy number *Da*, the buoyancy ratio *N* and the radius ratio on the fully developed natural convection heat and mass transfer in a vertical annular non-Darcy porous medium with asymmetric wall temperatures and concentrations, the effects of these three factors on the volume flow rate and the total heat and species rates were examined. Charrier-Mojtabi [12] carried out a numerical investigation of two dimensional and three-dimensional free convection flows in a saturated porous horizontal annulus heated from the inner surface. Chart and Hus [13] investigated numerical computations for turbulent mixed convection of air in a horizontal concentric annulus between a cooled outer cylinder and a heated, rotating inner cylinder. From the previous review, the double diffusion mixed convection in a rotating annulus is very important in many engineering applications. Therefore, the present investigation is devoted to study this configuration. The inner cylinder is isothermally heated and capable of rotating in the both directions; clockwise and anti-clockwise. Also the inner cylinder is considered to be a source for the concentration. On the other hand, the outer cylinder is considered fixed, isothermally cold and a sink for the concentration.

2. Mathematical model

Two long concentric horizontal cylinders with gab width, *b*, are considered. The geometry of the problem is shown in Fig. 1. Both of the two cylinders are held at constant but different temperatures and concentrations of T_i, C_i and T_o, C_o ($T_i > T_o$) and ($C_i > C_o$). The temperature gradient generates the natural thermal diffusive force and the concentration gradient generates the natural solutal diffusive force. The inner cylinder is considered able to rotate in clockwise and anti-

clockwise directions to create the forced convection. In addition, the flow in the annular region is assumed to be Newtonian, two-dimensional, steady and laminar. Also, all thermo-physical properties of the fluid are taken to be constant except for the density variation in the buoyancy term, where the Boussinesq approximation is considered to be linearly proportional to both temperature and concentration such that:

$$\rho = \rho_o[1-\beta_T(T-T_o)-\beta_S(C-C_o)] \quad (1)$$

Where β_T and β_s are the coefficients for thermal and concentration expansions, respectively such that:

$$\beta_T = -\frac{1}{\rho_o}\left(\frac{\partial\rho}{\partial T}\right)_{P,C} \text{ and } \beta_S = -\frac{1}{\rho_o}\left(\frac{\partial\rho}{\partial C}\right)_{P,T} \quad (2)$$

To put the governing equations in the dimensionless form, the following dimensionless variables are introduced to the governing equations.

$$V_r = \frac{v_r}{\omega r_i}, V_\varphi = \frac{v_\varphi}{\omega r_i},\ R = \frac{r}{b},\ \theta = \left(\frac{T-T_o}{T_i-T_o}\right),\ P' = \frac{p}{\rho(\omega r_i)^2},\ C' = \left(\frac{C-C_o}{C_i-C_o}\right) \quad (3)$$

The dimensionless form of governing equations for the continuity, momentum, thermal energy and species transport in the cylindrical coordinate are:

$$\left(\frac{\partial V_r}{\partial R}+\frac{V_r}{R}+\frac{\partial V_\varphi}{R\partial\varphi}\right)=0 \quad (4)$$

$$\left(V_r\frac{\partial V_r}{\partial R}+V_\varphi\frac{\partial V_r}{R\partial\varphi}-\frac{V_\varphi^2}{R}\right)=-\frac{\partial P'}{\partial R}-\frac{Gr_T}{\mathrm{Re}^2}((\theta+NC')\cos\varphi)+\frac{1}{\mathrm{Re}}\left(\frac{\partial^2 V_r}{\partial R^2}+\frac{1}{R}\frac{\partial V_r}{\partial R}-\frac{V_r}{R^2}+\frac{\partial^2 V_r}{R^2\partial\varphi^2}-\frac{2}{R^2}\frac{\partial V_\varphi}{\partial\varphi}\right) \quad (5)$$

$$\left(V_r\frac{\partial V_\varphi}{\partial R}+V_\varphi\frac{\partial V_\varphi}{R\partial\varphi}+\frac{V_rV_\varphi}{R}\right)=-\frac{\partial P'}{R\partial\varphi}+\frac{Gr_T}{\mathrm{Re}^2}((\theta+NC')\sin\varphi)+\frac{1}{\mathrm{Re}}\left(\frac{\partial^2 V_\varphi}{\partial R^2}+\frac{1}{R}\frac{\partial V_\varphi}{\partial R}-\frac{V_\varphi}{R^2}+\frac{\partial^2 V_\varphi}{R^2\partial\varphi^2}+\frac{2}{R^2}\frac{\partial V_r}{\partial\varphi}\right) \quad (6)$$

$$\left(V_r\frac{\partial\theta}{\partial R}+V_\varphi\frac{\partial\theta}{R\partial\varphi}\right)=\frac{1}{\mathrm{Re}\,\mathrm{Pr}}\left[\frac{1}{R}\frac{\partial}{\partial R}\left(R\frac{\partial\theta}{\partial R}\right)+\frac{\partial^2\theta}{R^2\partial\varphi^2}\right] \quad (7)$$

$$\left(V_r\frac{\partial C'}{\partial R}+V_\varphi\frac{\partial C'}{R\partial\varphi}\right)=\frac{1}{\mathrm{Re}\,S_C}\left[\frac{1}{R}\frac{\partial}{\partial R}\left(R\frac{\partial C'}{\partial R}\right)+\frac{\partial^2 C'}{R^2\partial\varphi^2}\right] \quad (8)$$

Where V_r, V_φ are the dimensionless velocity components in the radial and angular directions respectively, P' is the dimensionless pressure. $Re = \omega r_i\, b / \nu$, is the rotational Reynolds number, $N = Gr_S / Gr_T$ is the Buoyancy ratio, $Sc = \nu/D$ is the Schmidt number, $Pr = \nu/\alpha$ is the Prandtl number. Whereas $Gr_S = g\,\beta_S\,(c_i-c_o)\,b^3/\nu^2$ and $Gr_T = g\,\beta_T\,(T_i-T_o)\,b^3/\nu^2$ are the solutal and thermal Grashof numbers.

For the boundary conditions, the temperature and concentration gradients are maintained by considering higher magnitudes at the inner cylinder. In addition, the outer cylinder is fixed but the inner cylinder is assumed to rotate in clockwise and anti-clockwise directions.

The dimensionless boundary conditions for the anti-clockwise and clockwise rotations are:

$$V_\varphi = \pm 1, V_r = 0, \theta = 1.0 \text{ and } C' = 1.0, \text{ at } R = R_i \quad (9)$$

$$V_\varphi = 0, V_r = 0, \theta = 0 \text{ and } C' = 0, \text{ at } R = R_o \quad (10)$$

The positive sign refers to the anti-clockwise rotation where the negative sign refers to the clockwise rotation. By defining the Nusselt number as the ratio between the actual heat transfer rate and the heat transferred by pure conduction, then the local Nusselt number along the inner cylinder is calculated as:

$$Nu_\varphi = -\left(R\frac{\partial\theta/\partial R}{Nu_{cond}}\right)_{R=R_i} \quad (11)$$

Where Nu_{cond} is the Nusselt number in the case of heat transfer through the annulus by pure conduction and given by:

$$Nu_{cond} = \left(1/\ln\frac{R_o}{R_i}\right) \tag{12}$$

From equations (13) and (14), the final form of the local Nusselt number is as follows:

$$Nu = \ln\left(\frac{R_i}{R_o}\right)\times\left(R\frac{\partial\theta}{\partial R}\right)_{R=R_i} \tag{13}$$

The average Nusselt number is calculated from integrating the local value over the circumference of the inner cylinder as follows:

$$Nu = \frac{1}{2\pi}\int_0^{2\pi} Nu\, d\varphi. \tag{14}$$

Similarly, we can calculate both local and average Sherwood numbers as follows:

$$Sh = \ln\left(\frac{R_i}{R_o}\right)\times\left(R\frac{\partial C'}{\partial R}\right)_{R=R_i} \tag{15}$$

$$Sh = \frac{1}{2\pi}\int_0^{2\pi} Sh\, d\varphi. \tag{16}$$

3. Solution procedure

The governing equations were solved by using the finite volume technique developed by Patankar [14]. This technique was based on the discretization of the governing equations using the central differencing in space. Firstly the effect of the number of grids on the solution was examined. Fig. 2 shows the effect of number of grid on the solution. Through this study, the domain size was (92 × 72) used. A uniform grid distribution in both radial and circumferential directions was used. The discretization equations were solved by the Gauss–Seidel method. The iteration method used in this program is a line-by-line procedure, which is a combination of the direct method and the resulting Tri Diagonal Matrix Algorithm (TDMA). The convergence of the iteration is determined by the change in the average Nusselt and Sherwood numbers as well as other dependent variables through one hundred iterations to be less than 0.01% from its initial value. Fig. 3 shows the convergence and stability of the solution.

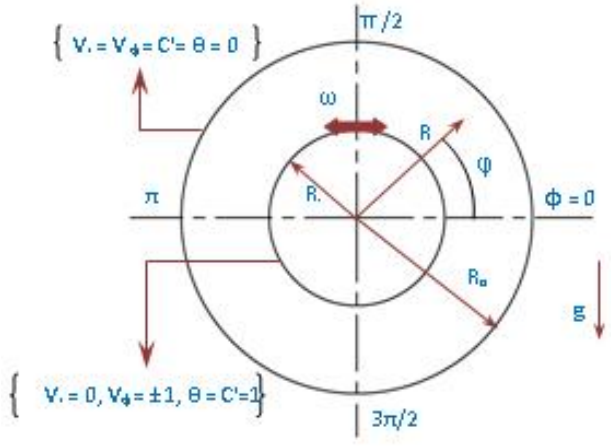

Figure.1. A Schematic Diagram of the Problem with Boundary Conditions

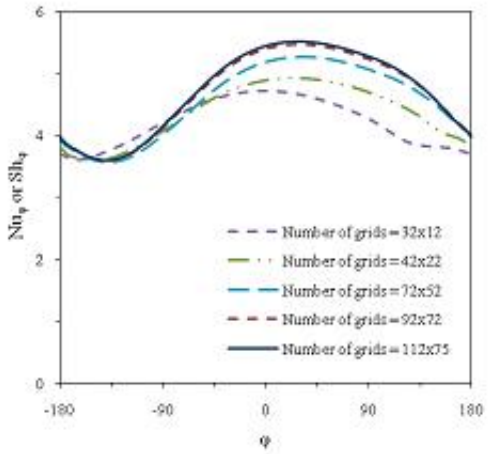

Figure 2. Convergence of the Local Nusselt and Sherwood Numbers at the Inner Cylinder for Pr = 50, Le =1, N =1 and Ri =1

4. Program validation and comparison with previous work

The results reported by Mohamed A. Teamah [9] on double diffusion mixed convection of air in rotating annulus were used to benchmark them against the outcome of our program. Fig. 4 plots the average Nusselt number over a range of buoyancy ratio from −20 to 20. Through the Fig., the thermal Rayleigh number was kept constant at $10^4$and rotational Reynolds number was kept constant at 100. The Fig. shows a comparison between the results obtained from the program used in this investigation and the results published by Mohamed A. Teamah [9] for Le =1 and Le = 5. The maximum deviation between the results was within 4%. In addition, the results are presented in Fig. 5 in terms of streamline and isotherm patterns where the inner cylinder was rotating in anti-clockwise direction and the outer cylinder was kept constant. The dimensionless temperature and concentration at the inner cylinder were kept constant and their values equal unity while their values at the outer cylinder equal to zero. In addition, the Prandtl number was kept constant at 0.7. The value of Lewis number and Buoyancy ratio were kept constant and equaled unity. As shown in Fig. 5, the comparisons for Ra_T = 10^3 and 10^4 are in excellent agreements, which provide sufficient confidence in the numerical algorithm.

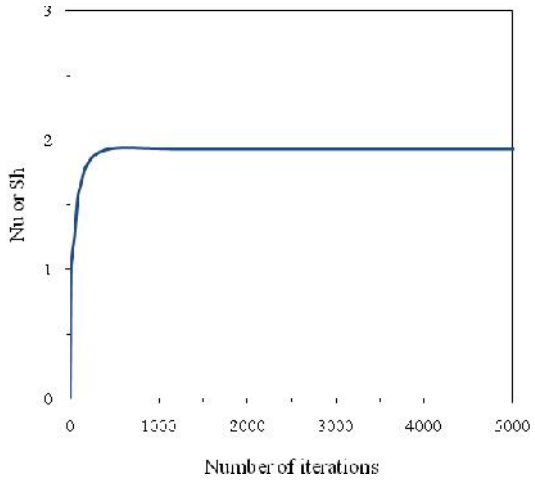

Figure 3. Average Nusselt and Sherwood Numbers Pr = 0.7, Le =1, N =1 and Ri =1

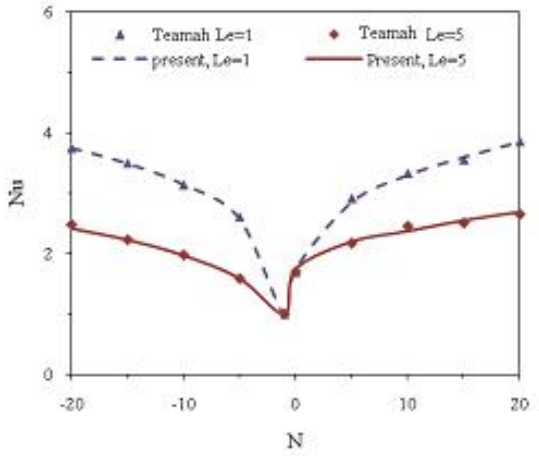

Figure 4. Comparison with Teamah [9], Anti-Clockwise Rotation, Re = 100, Ra = 10^4 and Pr = 0.7

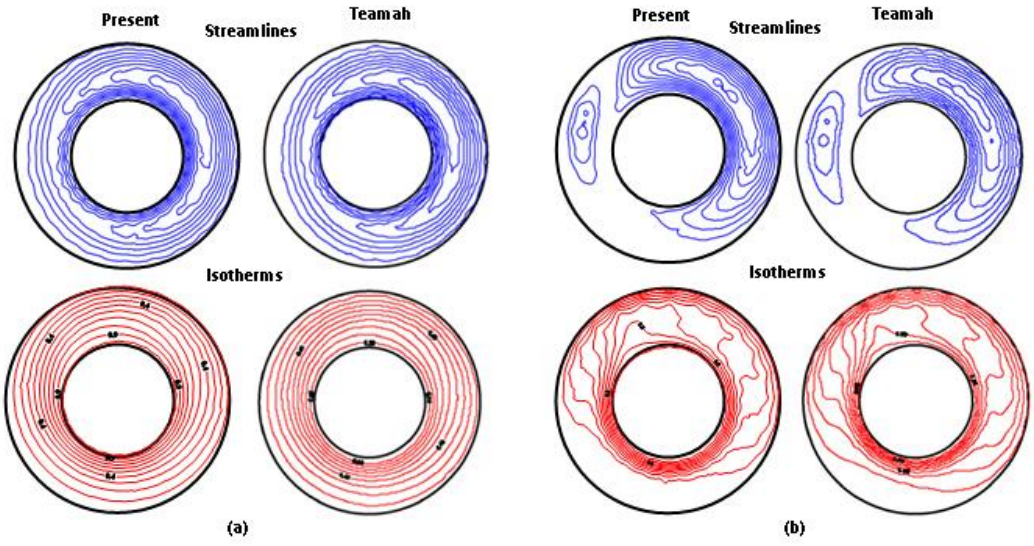

Fig. 5. Comparisons of the Streamlines and Isotherms between the Present Work and Teamah [9] For Pr = 0.7, N =1, Le =1, Re =100 and (a) Ra_T =10^3, (b) Ra_T =10^4

5. Results and discussion

Different scenarios were explored to explain the effects of different parameters on the studied problem. These two parameters are Richardson number and Lewis number. The results were obtained for the two cases of the inner cylinder rotation. The results were divided into local results and average results. In order to highlight the effect of Richardson number, Lewis number was kept constant at value equals one which means, the thermal diffusion equals the mass diffusion. Therefore, the isotherms are only presented. All results were performed with thermal Grashof number and radius ratio equaled to 10^4 and 2 respectively.

5.1. Effect of Richardson number

a. The inner cylinder rotates in anti-clockwise direction

The effect of the Richardson number on the streamlines and isotherms for the anti-clockwise direction is shown in Fig. 6(a). For high value of Richardson number (*Ri* =100), the flow is supposed to be induced by the buoyancy force sustained by the temperature gradient. The streamlines consists of one pair of cells, one at the right and another one at the left portion of the cavity. The two cells are not similar in shape. Since in the right portion the forced flow assisted the natural flow on the other hand in the left portions the two streams opposing each other, the right cell is stronger than the left cell. This destroys both the similarity of the two cells shape and their symmetry. The separation line of Ψ=0 which separates the two large eddies moves in the direction of the cylinder rotation. Both eddies circulate in opposite direction to each other. The right cell rotates in the direction of counter clockwise. As *Ri* is decreased the effect of forced flow is profound. In left portion, the eddy in that region becomes weaker and smaller. Conversely, in the other portion, the right eddy becomes stronger and bigger. Also, the separation line still moves in anti-clockwise direction and encompasses the small eddy. At *Ri* =1, the mixed convection is dominated, the right eddy becomes more bigger and fills the right portion of the annulus but is also deflected to the left at the top of the annulus due to the effect of the drag force. As *Ri* decreases, the viscous force drags the two cells in the direction of the cylinder rotation. At *Ri* = 0.1, the left eddy disappears and the flow pattern moves from two eddies towards one eddy and the separation line encompasses the large eddy again. At *Ri* =100, the forced flow is dominated, the remaining eddy disappears and the flow regime moves from one eddy towards no-eddy. The flow pattern becomes concentric circles around the inner cylinder. This distribution is similar to the couette flow patterns. The flow strength is very high close to the inner cylinder. Conversely, it is very weak nearer the outer cylinder. On the other hand, and for high Richardson number, the isotherms are represented by the thermal plume which appears over the inner cylinder and very closed isotherms under the inner cylinder which represented high rates of heat and mass transfer. As *Ri* decreases, the thermal plume rotates in the direction of the cylinder rotation and gets bigger in size. At *Ri* = 0.1, the thermal plume becomes so bigger and a wide gap is found between the isotherms close to the inner cylinder and the isotherms near the outer cylinder. As *Ri* decreases to 0.01(dominated forced convection regime), isotherms become almost concentric rings around the inner cylinder. Fig. 7(a) plots the local Nusselt and Sherwood numbers versus the angle for different Richardson number. From the figure, for *Ri* = 0.01, the forced flow dominated, the local Nusselt or Sherwood numbers are represented by approximately horizontal line. This means, the local Nusselt or Sherwood numbers are constant at any position around the inner cylinder. As *Ri* increases, natural flow is profound, both local Nusselt and Sherwood numbers increase. The maximum local Nusselt or Sherwood number is found under the inner cylinder and the minimum Local Nusselt or Sherwood numbers are found above the inner cylinder. As *Ri* increases, the points of the minimum and maximum local Nusselt and Sherwood numbers always move in the opposite direction of the cylinder rotation.

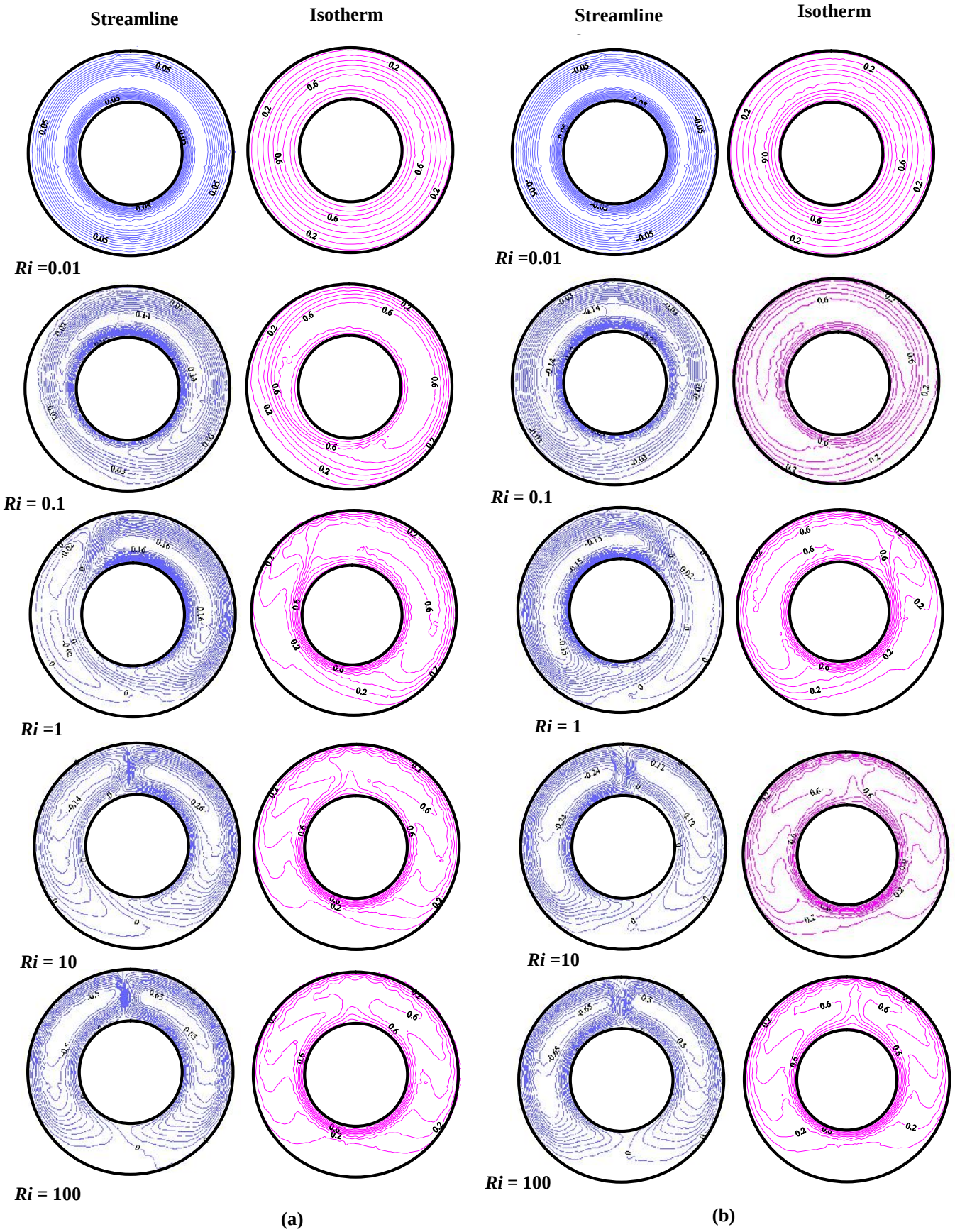

Figure 6. Effect of Richardson Number on the Streamlines and Isotherms for Le = 1, N = 1, Gr_T =10^4, Pr =6 and (a) Inner Cylinder Rotates in Anti-Clockwise, (b) Inner Cylinder Rotates Clockwise

b. The inner cylinder rotates in clockwise direction

The effect of the Richardson number on the streamlines and isotherms for the clockwise direction is shown in Fig. 6(b). In this case, the forced flow assisted the natural flow in the left portion of the cavity. Conversely, the two flows are opposing each other on the right portion. Therefore, same observations as discussed in the first case can be applied to explain figures (6b and 7b).

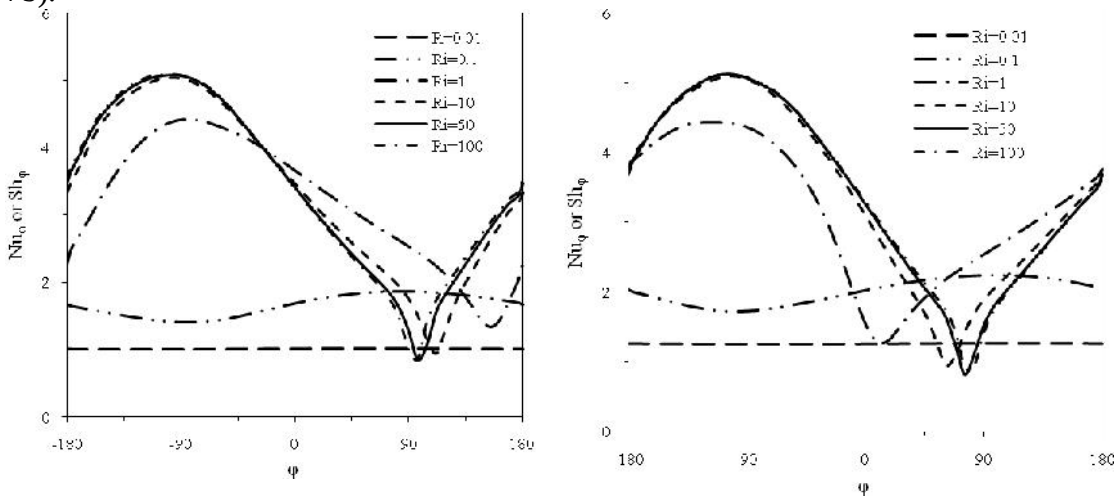

(a) (b)

Figure 7. Effect of Richardson Number on the Local Nusselt and Sherwood Numbers for Le = 1, N = 1, $Gr_T = 10^4$, Pr =6 and (a) Inner Cylinder Rotates in Anti-Clockwise, (b) Inner Cylinder Rotates in Clockwise Direction

5.2. Effect of Lewis number

a. The inner cylinder rotates in anti-clockwise direction

The effect of Lewis number on the streamlines, isotherms and iso-concentrations for the anticlockwise rotation is shown in Fig. 8 (a). At *Le* = 0.01, the mass diffusion is very high compared to the thermal diffusion and the thermal plume is found above the inner cylinder but the iso-concentrations are stratified in the radial directions. At *Le* = 0.1, the thermal plume is bigger than the one for *Pr* = 0.7 that was studied by Teamah [9] and as *Le* increased the mass plume becomes bigger until a gap space is formed at *Le* =10. The rotational effect moves the mass and thermal plume as well as the two cells in the direction of the rotation. As Lewis number increases, the mass transfer rate near the inner cylinder is increased due to the decrease of mass diffusion. This is beneficial when a drying process is involved. The small eddy is almost disappeared at *Le* = 10. For *Le* > 1 and as *Le* increases, there is an invisible significant effect on the isotherms but for *Le* < 1, the thermal plumes tend to ease a bit with the increase in *Le* value. The dependence of both local Nusselt and Sherwood numbers over the circumference of the inner cylinder on the Lewis number is displayed in Fig. 9. For very small value of Lewis number, *Le* = 0.01, the local Sherwood number is almost constant around the inner cylinder and as Lewis number increases, the local Sherwood number increases. On the other hand, the local Nusselt slightly dips as the Lewis number increases. The predicted local Nusselt and Sherwood numbers have minimum values at the thermal plume angle which locates in the second quarter of the annulus. Furthermore, they have maximum values in opposite to the position of minimum values. As *Le* increases, the minimum and maximum points of the local Sherwood number rotate in anti-clockwise direction and the difference between the minimum and maximum points decreases until *Le* = 100, we can noticed a small difference between them.

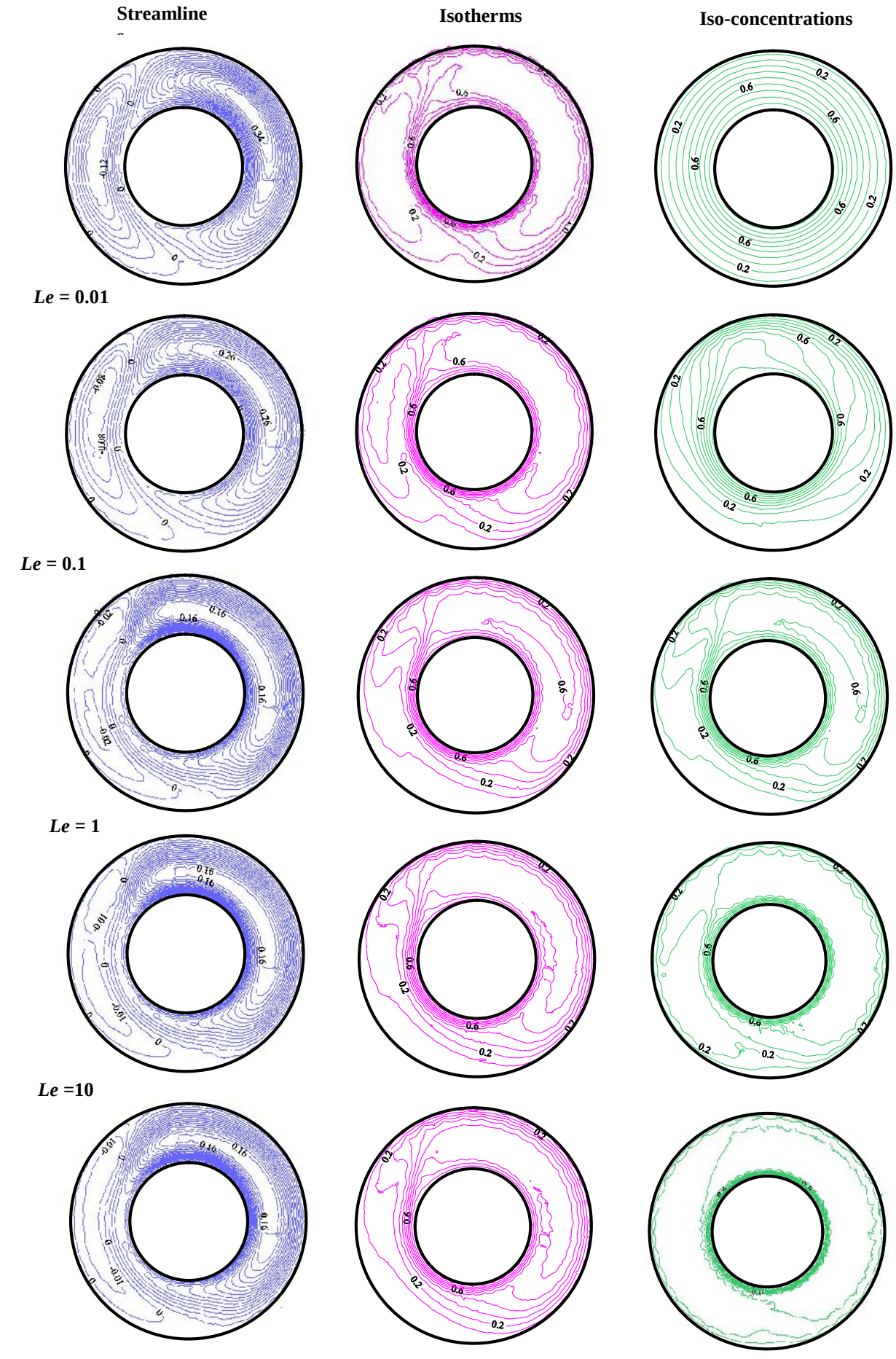
Streamline
Isotherms
Iso-concentrations
Le = 0.01
Le = 0.1
Le = 1
Le =10
Le = 100

(a)

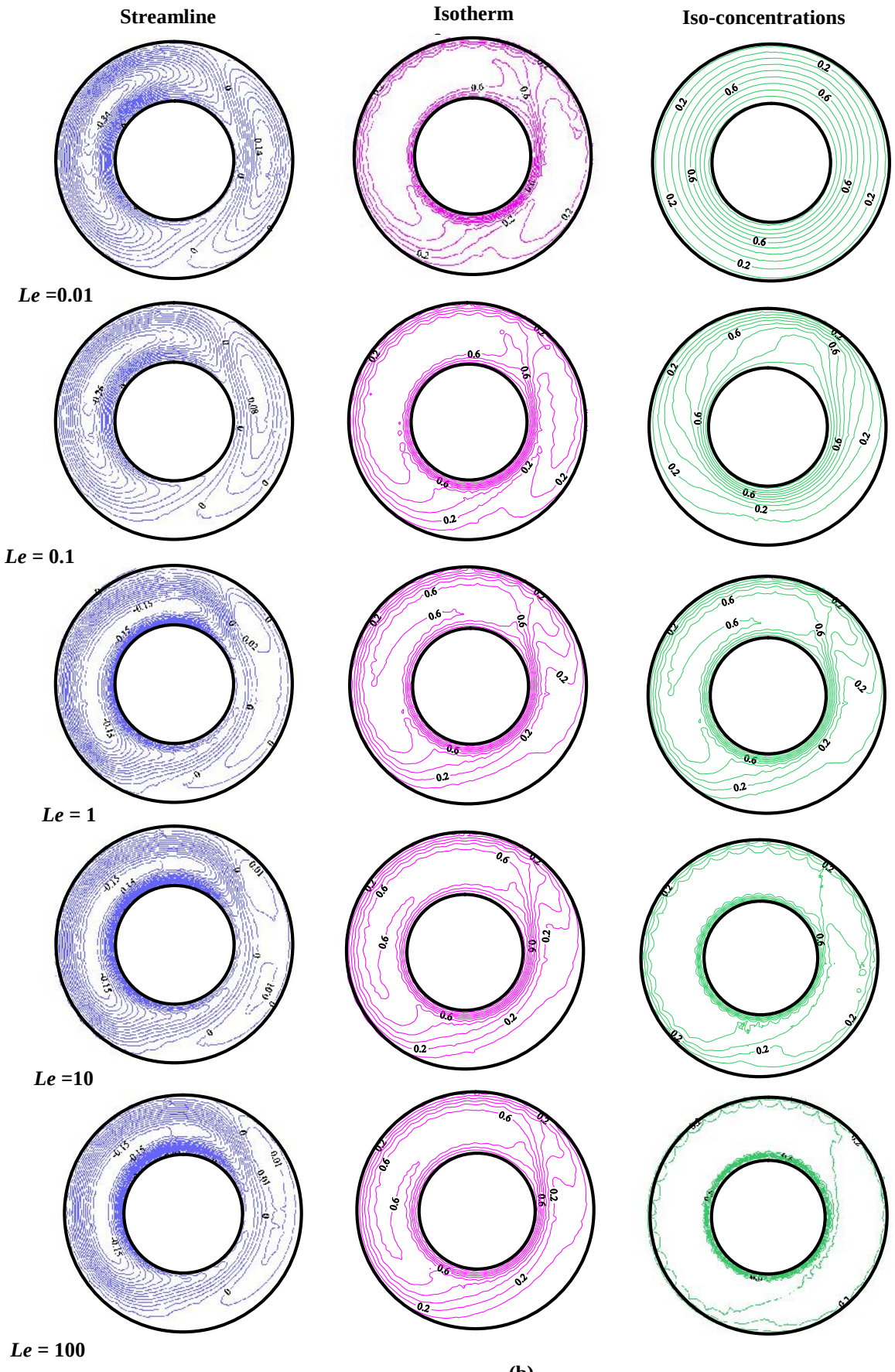

(b)

Figure 8. Effect of Lewis Number on the Streamlines and Isotherms for N = 1, Ri = 1, $Gr_T = 10^4$, Pr = 6 and (a) Inner Cylinder Rotates in Anti-Clockwise, (b) Inner Cylinder Rotates in Clockwise Direction

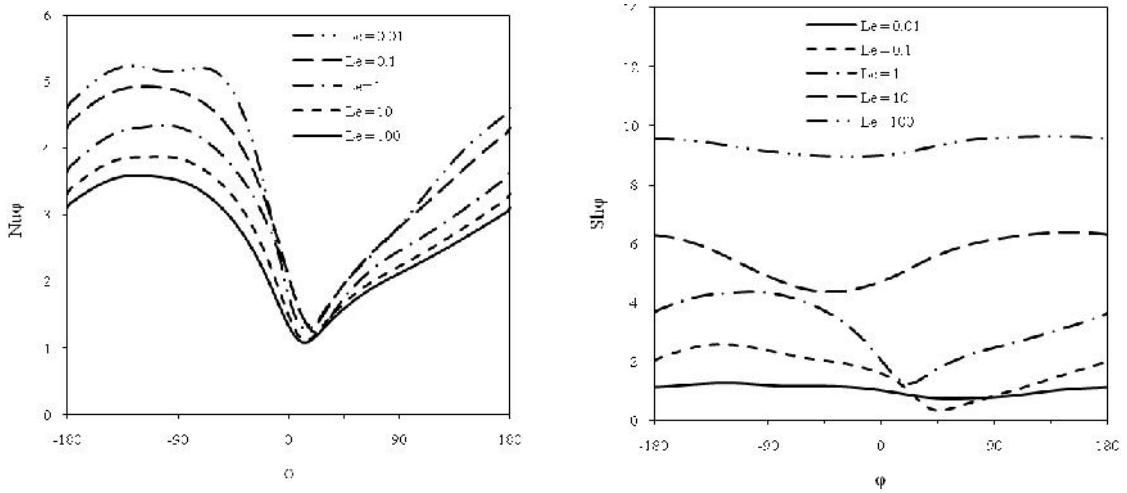

Figure 9. Effect of Lewis Number on the Local Nusselt and Sherwood Numbers for N = 1, Ri = 1, $Gr_T = 10^4$, Pr = 6 and (a) Inner Cylinder Rotates in Anti-Clockwise (b) Inner Cylinder Rotates in Clockwise Direction

b. The inner cylinder rotates in clockwise direction

The effect of Lewis number on the streamlines, isotherms and iso-concentrations for the clockwise rotation is shown in Fig. 8 (b). The flow, isothermal and iso-concentration patterns have a reversal behavior to those for the rotation in anti-clockwise direction but for the clockwise rotation, the streamlines, isotherms and iso-concentrations strength increases than those for the anti-clockwise rotation.

5.1. Effect of both Richardson and Lewis numbers

Figs. (10-11) show the effect of Lewis number on the average Nusselt and Sherwood numbers at different Richardson number. The results are computed for Lewis number ($0.01 \leq Le \leq 100$), for values of Richardson number of: 0.01, 0.1, 1 and 10. Through these results, Buoyancy ratio was fixed and equaled to one, Prandtl number was fixed at value equaled to 6 and the thermal Grashof number was fixed at value equaled to 10^4. The following remarks can be concluded:

- At constant Pr and Ri, as Le increases, the average Sherwood number increases. On the contrary, the Nusselt number predictions show a slight dip and then assume an asymptotic value with the increase in Le. Unlike the mass transfer enhancement, the transport of energy is not improved with the increase in Le value. Also, the predictions of the Nusselt and Sherwood numbers are coincided at Le = 1 giving the similarity in their diffusion characteristics.
- For forced convection flow (Ri < 1) and at constant value of Le, the clockwise rotation gives better heat and mass transfer than the other rotation for the double diffusive problem and this difference increases as Pr increases and Ri decreases.
- For constant Pr and for dominated forced convection regime (Ri = 0.01), as Le increases, there is no profound effect of Lewis number on the heat transfer for both directions of the inner cylinder rotation.
- For constant Pr and for dominated forced convection regime (Ri = 0.01), as Le increases, there is no profound effect of Lewis number on the mass transfer for the anti-clockwise rotation but for the clockwise rotation, the effect of Le on the average Sherwood is profound.
- As Ri decreases, the effect of Le on both heat and mass transfer increases and becomes more profound.

- For dominated mixed convection regime, and for Le < 0.05, there is no profound effect of Lewis number on both heat and mass transfer
-

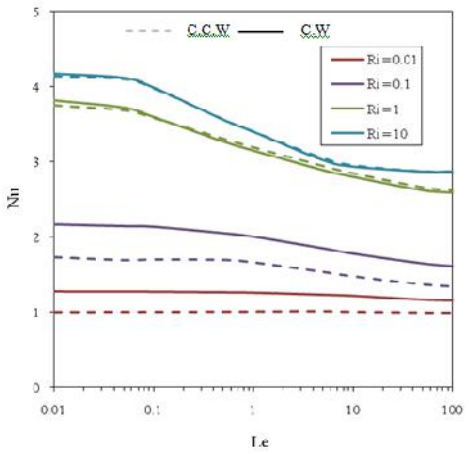

Figure 10. Combined Effect of Richardson Number and Lewis Number on the average Nusselt Number for N=1, $Gr_T = 10^4$ and Pr = 6

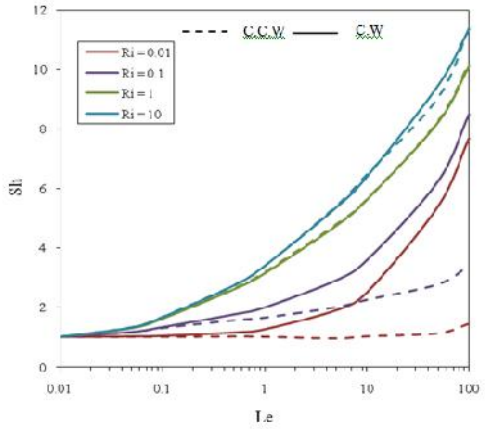

Figure 11. Combined Effect of Richardson Number and Lewis Number on the Average Sherwood Number for N = 1, $Gr_T = 10^4$ and Pr = 6

6. Conclusion

This investigation is concerned with the numerical simulation of double diffusive flow in a two-dimensional horizontal annulus with the inner cylinder rotating at clockwise and anti-clockwise directions. For the dominated forced convection regime, the local Nusselt and Sherwood numbers are kept at constant value around the inner cylinder. For both directions of the cylinder rotation, the points of the minimum and maximum local Nusselt and Sherwood numbers always move in the opposite direction of the cylinder rotation as Richardson number increases. The effect of the Lewis number on the local Nusselt number is not profound but as Lewis increased, the Local Sherwood number increased and the effect is more profound. For both directions, the minimum points of the local Sherwood number rotate in the same cylinder direction. As Lewis number increased, the mass transfer increased but no enhancement had happened for the heat transfer, this is beneficial when a drying process is involving. As Richardson number decreases, the clockwise rotation gives better heat and mass transfer compared to the other direction.

References

[1] Joo-Sik Yoo, Mixed convection of air between two horizontal concentric cylinders with a cooled rotating outer cylinder, Int. J. Heat Mass Transfer, 41(1998) 293-302.

[2] Joo Sik Yoo, Transition and multiplicity of flows in natural convection in a narrow horizontal cylindrical annulus: Pr=0.4, Int. J. Heat Mass Transfer, 42 (1999) 709-722.

[3] Joo Sik Yoo, Prandtl number effect on transition of free convection flows in a wide gap horizontal annulus, Int. Comm. Heat Mass Transfer, 26 (1999) 811-817.

[4] Gilles Desrayaud, Guy Lauriat, Pierre Cadiou, Thermoconvective instabilities in a narrow horizontal air-filled Annulus, Int. J. Heat Fluid Flow, 21(2000) 65-73.

[5] F. A. Hamad, M. K. Khan, Natural convection heat transfer in horizontal and inclined annuli of different diameter ratios, Energy Convers. Mgmt 39 (1998), 797-807.

[6] Y.D. Zhu, C. Shu, J. Qiu, J. Tani, Numerical simulation of natural convection between two elliptical cylinders using DQ method, Int. J. Heat Mass Transfer, 47(2004) 797–808.

[7] E. Abu-Nada, Z. Masoud, A. Hijazi, Natural convection heat transfer enhancement in horizontal concentric annuli using nanofluids, Int. Comm. Heat Mass Transfer, 35 (2008) 657–665.

[8] J.A. Bowman, D. T. Schwartz, High Peclet number mass transfer in the acoustic streaming flow between two concentric cylinders, Int. J. Heat Mass Transfer, 41(1998), 1065-1074.

[9] M. A. Teamah, Numerical simulation of double diffusive laminar mixed convection in a horizontal annulus with hot, solutal and rotating inner cylinder, Int. J. Thermal Sciences, 46 (2007) 637–648.

[10] K. Khanafer, A. J. Chamkha, Mixed convection within a porous heat generating horizontal annulus, Int. J. Heat Mass Transfer, 46 (2003) 1725–1735.

[11] C.Y. Cheng, Fully developed natural convection heat and mass transfer in a vertical annular porous medium with asymmetric wall temperatures and concentrations, Applied Thermal Engineering, 26 (2006) 2442–2447.

[12] M.C.Charrier-Mojtabi, Numerical simulation of two- and three dimensional free convection flows in a horizontal porous annulus using a pressure and temperature formulation, Int. J. Heat Mass Transfer, 40 (1997), 1521-1533.

[13] M. I. Chart, Y.H. Hsu, Numerical prediction of turbulent mixed convection in a concentric horizontal rotating annulus with low-Re two equation models, Int. J. Heat Mass Transfer, 41 (1998), 1633-1643.

[14] S.V.Patankar, Numerical Heat transfer and Fluid flow, McGRAW-HILL, New York, 1980.

Nomenclature

b	annulus gab width $b=(r_o-r_i)$, m.
C	concentration.
C'	dimensionless vapour concentration.
C_i' , C_o'	dimensionless concentrations at inner and outer radii respectively.
D	mass diffusivity, m^2/s.
g	acceleration of gravity,m/s^2.
Gr_S	solutal Grashof number based on the gab width.
Gr_T	thermal Grashof number based on the gab width.
h	heat transfer coefficient ,W/m^2 K.
h_s	solutal transfer coefficient, m/s.
K	fluid thermal conductivity, W/m K.
Le	Lewis number, Le = α/D.
N	Buoyancy ratio.
Nu	average Nusselt number.
Nu_φ	local Nusselt number.
P	pressure, N/ m^2.
P'	dimensionless pressure
Pr	Prandtl number.
r	radial coordinate.
r_i , r_o	inner and outer radii respectively, m
R	dimensionless radial coordinates.
Ri	Richardson number, $Ri=Gr/Re^2$.
Ra_S	solutal Rayleigh number based on the gab width.
Ra_T	thermal Rayleigh number based on the gab width.
Re	rotational Reynolds number.
Sc	Schmidt number.
Sh	average Sherwood number.
Sh_φ	local Sherwood number.
T	local temperature, K.

T_i , T_o	temperatures at inner and outer radii respectively, K.
ΔT	temperature difference, ($T_i - T_o$), K.
u	velocity vector, m/s.
U	dimensionless velocity vector.

Greek symbols

β_T	Coefficient of thermal expansion, K^{-1}.
β_S	Coefficient of solutal expansion, Kg^{-1}.
$\tilde{\alpha}$	Thermal diffusivity, m^2/s.
φ	angular coordinate
ω	angular velocity, rad/s.
ψ	dimensionless stream function
θ	dimensionless temperature.
ν	Kinematic viscosity, m^2/s.
ρ_o	Fluid density, Kg/m^3.